ISBN: 978-3-95450-247-9 ISSN: 2673-5490 doi: 10.18429/JACoW-IPAC2024-TUPS37

SHOWER SIMULATIONS FOR THE CERN PROTON SYNCHROTRON INTERNAL DUMP AND POSSIBLE SHIELDING OPTIONS

S. Niang*, L. S. Esposito, M. Giovannozzi, A. Huschauer, T. Pugnat
CERN, Geneva, Switzerland

Abstract

During the Long Shutdown 2, the two internal dumps were replaced and successfully integrated into the CERN Proton Synchrotron operation to withstand the intense and bright beams for the High-Luminosity LHC. They function as safety devices, designed to swiftly intersect the beam's trajectory and effectively stop the beam over multiple turns. A significant challenge arises from the limited energy absorption capacity. Previous studies indicate that at the maximum PS beam energy of 26 GeV, only about 6% of the energy is absorbed by the dumps upon their activation. This study, employing a combination of the FLUKA and SixTracksimulation code chain, evaluates the absorbed dose in downstream elements in view of the projected increase of beam intensities, according to the LHC injector upgrade parameters, and explores the feasibility and potential benefits of implementing shielding as a mitigation measure.

INTRODUCTION

The internal beam dumps of the CERN Proton Synchrotron (PS), located in straight sections (SS) 47 and 48, referred to as TDI.47 and TDI.48, were fully redesigned for installation during Long Shutdown 2 (LS2, 2019-2021). This redesign aimed to adapt the dump capabilities with the increase in beam brightness following the LHC Injector Upgrade (LIU) project [1, 2]. Once activated, this device moves rapidly into the beam and intercepts it in several turns (on the order of a few milliseconds) to protect the PS hardware against beam-induced damage. During the design phase, comprehensive studies confirmed the thermomechanical robustness of the new dump design [3–5] and evaluated its effectiveness in stopping post-LS2 PS beams [6].

In previous studies we described the simulation model, the performance of the dump [7], and validated the model with Beam Loss Monitor (BLM) data [8]. The implemented model used multiturn beam dynamics simulations conducted with Sixtrack [9, 10] to calculate impacts on the internal dumps while they move into the beam distribution. Subsequently, these impacts become the input of another simulation using FLUKA [11–13] for shower simulations to assess the effects of the radiation field on downstream equipment along the circumference of the PS ring from SS47 to SS69. These precedent studies assumed that the two internal dumps stop a total of 2.4×10^{17} protons per year, according to the functional specification [14]. Moreover, the case of the lead ion beam was not considered.

* samuel.niang@cern.ch

In this study, our aim is to detail the specific breakdown of particles (type and energy) that actually impacted the dumps during the 2023 run, enabling a more precise estimation of the dose absorbed by the main magnets. Recognising the vulnerability of epoxy-based elements installed in these magnets, we have improved our FLUKA model to include the front part of the coils of the initial magnets and the Pole Face Windings (PFW) circuits, which are used to control the PS working point, i.e. tunes and chromaticities (see Ref. [15] and references therein), as illustrated in Fig. 1. These components are primarily composed of copper and epoxy [16].

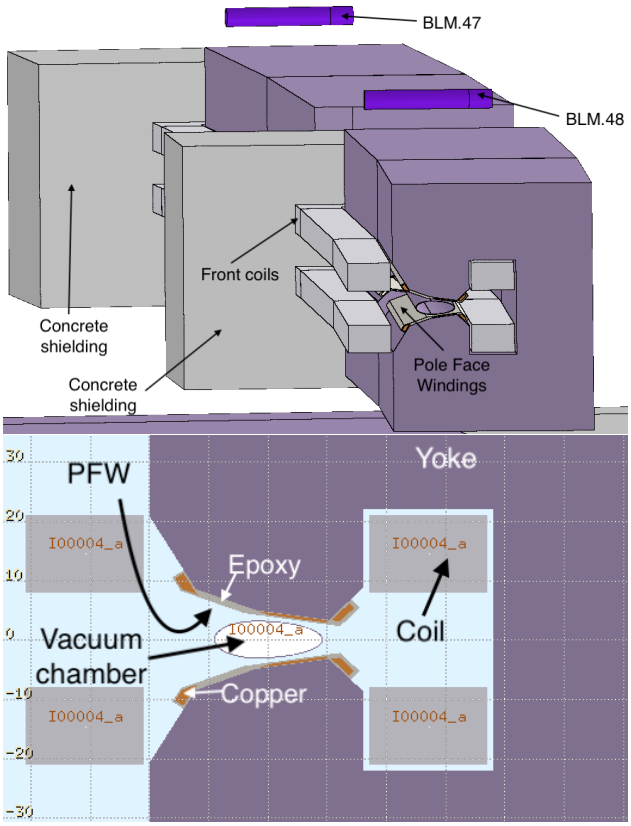

Figure 1: Visualisation, with FLAIR [17], of the FLUKA model.

BREAKDOWN OF THE PROPERTIES OF THE BEAM INTERCEPTED BY THE DUMPS

Using data from the NXCALS database [18], we analysed the operational use of the PS internal beam dumps during the entire 2023 run. The data, summarised in Table 1, show how

ISBN: 978-3-95450-247-9 ISSN: 2673-5490 doi: 10.18429/JACoW-IPAC2024-TUPS37

many times the internal dumps have been activated, and the number of charged particles they intercepted. An interesting finding from this analysis is the uneven use of the two dumps. TDI.47 was used 70% more than TDI.48, indicating a strong operational imbalance. This might have an impact on the mechanical stress in the dumps. However, it is worth noting that the total beam intensity stopped by the dumps is also very strongly unbalanced, but in the opposite direction. In fact, TDI.47, although activated more frequently than TDI.48, intercepted much less beam.

Table 1: Summary of the use of the internal dumps in terms of movements performed and total intensity stopped by the internal dumps in 2023.

	TDI.47		TDI.48	
	Counts	Charges	Counts	Charges
Protons	25313	1.76×10^{16}	72637	7.86×10^{16}
Pb^{54+}	100550	1.78×10^{15}	1	2.22×10^{10}
Total	125861		72638	

Starting by the case of the proton beams, the actual number of protons intercepted by the two internal dumps was 9.62×10^{16}, which is significantly lower than the 2.4×10^{17} protons previously estimated in Ref. [14], a discrepancy of approximately 2.5 times. This difference is justified by the fact that the HL-LHC beams are already available in the injectors, but not yet delivered to the upgraded LHC ring. In particular, TDI.48 stopped about 82% of the protons. Figure 2 illustrates the distributions of the number of protons intercepted by the internal dumps as a function of the beam momentum. In particular, most protons are concentrated at a momentum of 26 GeV/c considering the sum of the two dumps. Hence, for the purposes of this study, we will assume that 8×10^{16} protons per year (i.e. approximately the number of protons stopped by TDI.48 in the 2023 run) with a momentum of 26 GeV/c are intercepted by a dump. This is a conservative estimate of the present situation. We checked that the contribution to the dose from lower-energy protons is smaller than that at top energy.

For the case of Pb^{54+} ion beams, almost all 3.30×10^{13} ions dumped were intercepted by TDI.47. Fig. 3 shows the distribution of the number of stopped ions as a function of the beam momentum, which shows three groups centred around 351.9, 578.1, and 794.4 GeV/c. Consequently, we will model the interaction of 3.30×10^{13} ions per year with a momentum of 578.1 GeV/c (corresponding kinetic energy of 2 GeV per nucleon) as representative of operational conditions during the 2023 run.

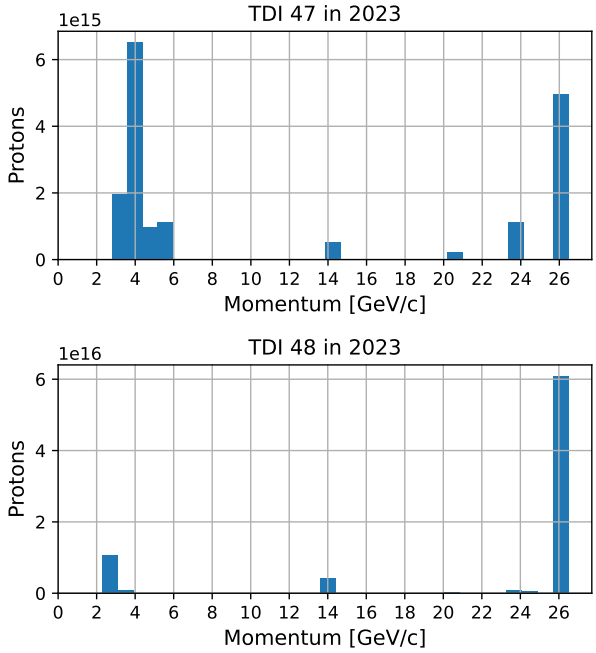

Figure 2: Distribution of the protons sent on the internal dumps in the 2023 run as a function of the beam momentum.

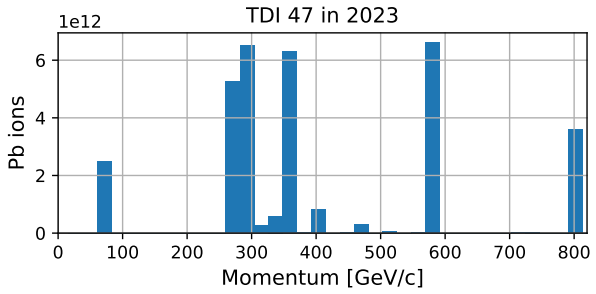

Figure 3: Distribution of the Pb^{54+} ions sent on TDI.47 in the 2023 run as a function of the beam momentum.

ABSORBED DOSE

Under the assumption that 8×10^{16} protons are intercepted by TDI.47, the data shown in Fig. 4 indicate that the absorbed dose from the interaction between the protons and the dump will not exceed 0.2 MGy per year in the most sensitive areas of the main unit magnets. Specifically, the front part of the coils in the main unit 47 receives a dose of 0.03 MGy, while those in the main unit 48 absorb ten times less dose. These data demonstrate that the current shielding of the internal dumps adequately protects the most vulnerable components, which are primarily made of epoxy and can tolerate an accumulated dose of up to 10 MGy [19]. This level of shielding effectiveness is contingent on maintaining the current proton dump rates; however, even if the proton count were increased to the level initially expected 2.4×10^{16} protons on target, the maximum absorbed dose would still remain well below 0.6 MGy.

However, if we look at the dose at the front face of the magnet following TDI.47 we observe that the dose in the epoxy part of the PFW exceeds locally 1 MGy per year for 8×10^{16} protons stopped by TDI.47. This is why we recommend conducting annual inspections of the PFWs to monitor for any signs of degradation.

In the case of lead ions, we consider a scenario in which TDI.47 stops 3.30×10^{13} ions per year with a momentum

ISBN: 978-3-95450-247-9 ISSN: 2673-5490 doi: 10.18429/JACoW-IPAC2024-TUPS37

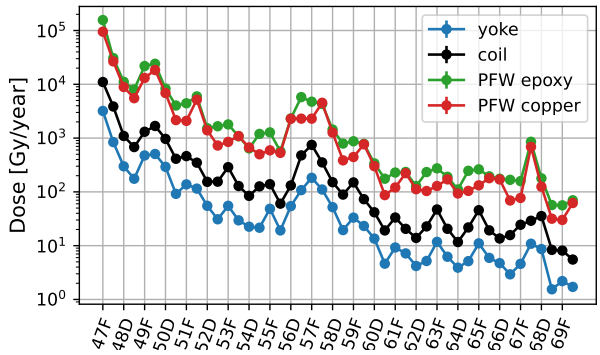

Figure 4: Total yearly integrated dose delivered to the yoke, coils, and PFWs of the PS main magnets. An operational year, assuming 8×10^{16} protons are stopped by TDI.47 at 26 GeV/c, has been considered. The F and D letters refer to the focusing and defocusing half-unit of each magnet, respectively. In these simulations, we considered the component of the PFWs installed in the upper pole of the magnet.

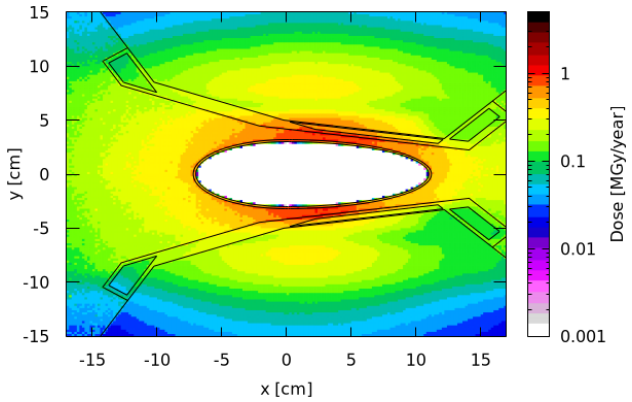

Figure 5: Dose absorbed by the front face of the main unit magnet 47 (right downstream of TDI.47). The integration along the longitudinal variable z was calculated over a span of 10 cm.

of 578.1 GeV/c. In the FLUKA simulations, full heavy-ion transport settings were enabled including ion electromagnetic dissociation interactions. Given that numerical simulations with ions are significantly more time consuming than those for protons, and the expected results should have minimal impact on the conclusions, given the very low beam intensities, we limited the scope of our simulations to the case of TDI.47, considering only the ring section from SS47 to Straight SS49. This includes the first three main magnet units downstream of the dumps. The absorbed doses are detailed in Fig. 6.

The data indicate that the maximum dose absorbed by PFWs in the case of lead ions remains below 1 kGy per year. Specifically, the front coil of main unit 47 receives a dose of 0.13 kGy per year, while the front part of the coil in main unit 48 receives ten times less. This confirms that the contribution of lead ions to the total absorbed dose absorbed by the various components is negligible.

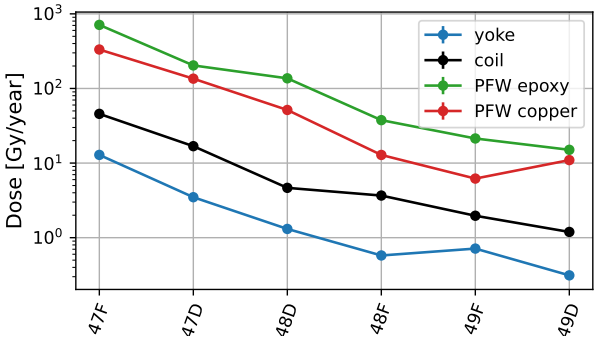

Figure 6: Total yearly integrated dose in the yoke, coils, and PFWs of the PS main magnets. An operational year, assuming 3.30×10^{13} ions with a momentum of 578.1 GeV/c are stopped by TDI.47, has been considered. The F and D letters refer to the focusing and defocusing half-unit of each magnet, respectively. In these simulations, we considered the component of the PFWs installed in the upper pole of the magnet.

CONCLUSIONS

In this study, we have performed FLUKA simulations to estimate the dose absorbed by the main magnet components of the PS ring during the actuation of the internal dumps, considering different beam particle type, energy, and intensity.

Based on the 2023 run operations data, we have assessed the contribution of the different beams. We have documented that during 2023, the number of protons directed at the internal dumps was 2.5 times lower than expected from the specification document. Additionally, the utilisation of the TDIs devices was uneven: the majority of protons were stopped using TDI.48, while all lead ion beams were stopped by TDI.47. This distribution imbalance suggests the need for future rebalancing if we want to avoid premature ageing of one dump compared to another.

With respect to radiation shielding, the estimated accumulated dose values are tolerable by the different magnet components. This conclusion remains valid even if the number of stopped protons is increased to the planned levels. However, our analysis of the worst-case scenario indicates that the epoxy components of the PFWs in the main units 47 and 48 are more susceptible to radiation exposure than other parts. This exposure could potentially reach the deterioration threshold within a decade. Therefore, we recommend annual inspections of these elements to prevent critical degradation and ensure ongoing safety and system functionality.

ACKNOWLEDGEMENTS

We would like to thank D. Bodart for providing valuable updates regarding the magnets, and F.-X. Nuiry for offering insightful perspectives on previous studies.

ISBN: 978-3-95450-247-9 ISSN: 2673-5490 doi: 10.18429/JACoW-IPAC2024-TUPS37

REFERENCES

[1] H. Damerau *et al.*, *LHC Injectors Upgrade, Technical Design Report*. CERN, 2014, doi:10.17181/CERN.7NHR.6HGC

[2] *LHC Injector Upgrade Project*, https://espace.cern.ch/liu-project/default.aspx.

[3] J. A. B. Monago *et al.*, "Multi-turn Study in FLUKA for the Design of CERN-PS Internal Beam Dumps," in *Proc. IPAC'18*, Vancouver, Canada, Apr.-May 2018, pp. 724–727, doi:10.18429/JACoW-IPAC2018-TUPAF025

[4] G. Romagnoli *et al.*, "Design of the New PS Internal Dumps, in the Framework of the LHC Injector Upgrade (LIU) Project," in *Proc. IPAC'17*, Copenhagen, Denmark, May 2017, pp. 3521–3523, doi:10.18429/JACoW-IPAC2017-WEPVA109

[5] G. Romagnoli *et al.*, "Engineering Design and Prototyping of the New LIU PS Internal Beam Dumps," in *Proc. IPAC'18*, Vancouver, Canada, Apr.-May 2018, pp. 2600–2603, doi:10.18429/JACoW-IPAC2018-WEPMG001

[6] R. Steerenberg and D. Cotte, "PS Beam Spot Sizes for the Design of New Internal Beam Dumps," CERN, Tech. Rep., 2017, https://edms.cern.ch/ui/file/1612293/1/PS_Beam_Size_Calculations_InternalDumps.pdf

[7] T. Pugnat *et al.*, "Study of the Performance of the CERN Proton Synchrotron Internal Dump," in *Proc. 68th Adv. Beam Dyn. Workshop High-Intensity High-Brightness Hadron Beams (HB'23)*, Geneva, Switzerland, Oct. 9–13, 2023, 2024, pp. 555–558, doi:10.18429/JACoW-HB2023-THBP36

[8] S. Niang *et al.*, "Shower Simulations for the CERN Proton Synchrotron Internal Dump and Comparison with Beam Loss Monitor Data," in *Proc. 68th Adv. Beam Dyn. Workshop High-Intensity High-Brightness Hadron Beams (HB'23)*, Geneva, Switzerland, Oct. 9–13, 2023, 2024, pp. 389–392, doi:10.18429/JACoW-HB2023-THC2C1

[9] R. De Maria *et al.*, SixTrack – *6D Tracking Code*, http://sixtrack.web.cern.ch/SixTrack/.

[10] R. D. Maria *et al.*, "SixTrack Version 5: Status and New Developments," in *Proc. IPAC'19*, Melbourne, Australia, May 2019, pp. 3200–3203, doi:10.18429/JACoW-IPAC2019-WEPTS043

[11] https://fluka.cern

[12] G. Battistoni *et al.*, "Overview of the FLUKA code," *Ann. Nucl. Energy*, vol. 82, pp. 10–18, 2015, doi:10.1016/j.anucene.2014.11.007

[13] C. Ahdida *et al.*, "New capabilities of the FLUKA multi-purpose code," *Front. Phys.*, vol. 9, 2022, doi:10.3389/fphy.2021.788253

[14] F.-X. Nuiry and G. Romagnoli, "PS Ring Internal Dumps Functional Specifications," CERN, Tech. Rep., 2017, https://edms.cern.ch/ui/file/1582110/2.1/PS-TDI-ES-0001-20-10.pdf

[15] J.-P. Burnet *et al.*, *Fifty years of the CERN Proton Synchrotron: Volume 1*. CERN, 2011, doi:10.5170/CERN-2011-004

[16] P. Freyermuth *et al.*, "CERN Proton Synchrotronworking point Matrix for extended pole face winding powering scheme," 2010, https://cds.cern.ch/record/1287599

[17] V. Vlachoudis, "Flair: A powerful but user friendly graphical interface for FLUKA," in *Proc. Int. Conf. on Mathematics, Computational Methods & Reactor Physics (M&C 2009)*, 2009, https://cds.cern.ch/record/2749540

[18] J. Wozniak and C. Roderick, "NXCALS - Architecture and Challenges of the Next CERN Accelerator Logging Service," in *Proc. ICALEPCS'19*, New York, NY, USA, 2020, pp. 1465–1469, doi:10.18429/JACoW-ICALEPCS2019-WEPHA163

[19] P. Beynel, P. Maier, and H. Schönbacher, *Compilation of radiation damage test data. Index des résultats d'essais de radiorésistance*. CERN, 1982, doi:10.5170/CERN-1982-010